Experimental and Theoretical Investigations of the Formation of the Diazene PhSN═C(H)N═NC(H)═NSPh from $HCN_2(SPh)_3$ by a Thiyl-Radical-Catalyzed Mechanism: Identification of the $HC(NSPh)_2^{\bullet}$ Radical and X-ray Structures of $HCN_2(SPh)_3$ and PhSN═C(H)N═NC(H)═NSPh

Tristram Chivers,*,† Bruce McGarvey,‡ Masood Parvez,† Ignacio Vargas-Baca,† and Tom Ziegler†

Department of Chemistry, The University of Calgary, Calgary, Alberta, Canada T2N 1N4, and Department of Chemistry and Biochemistry, University of Windsor, Windsor, Ontario, Canada N9B 3P4

Received March 22, 1996[⊗]

The reaction of $HCN_2(SiMe_3)_3$ with benzenesulfenyl chloride in a 1:3 molar ratio produces $HCN_2(SPh)_3$ (**4**) as thermally unstable, colorless crystals. The decomposition of (**4**) in toluene at 95 °C was monitored by UV−visible, ^{1}H NMR and ESR spectroscopy. The major final products of the decomposition were identified as PhSN═C(H)N═NC(H)═NSPh (**5**) and PhSSPh. The structures of **4** and **5** were determined by X-ray crystallography. The crystals of **4** are monoclinic, space group $P2_1/a$, with $a = 9.874(2)$ Å, $b = 19.133(2)$ Å, $c = 10.280(2)$ Å, $\beta = 113.37(1)°$, $V = 1782.8(5)$ Å^3, and $Z = 4$. The final R and R_w values were 0.042 and 0.049, respectively. The crystals of **5** are monoclinic, space group $P2_1/n$, with $a = 5.897(6)$ Å, $b = 18.458(10)$ Å, $c = 7.050(8)$ Å, $\beta = 110.97(5)°$, $V = 716(1)$ Å^3, and $Z = 2$. The final R and R_w values were 0.075 and 0.085, respectively. The diazene **5** adopts a *Z,E,Z* structure with weak intramolecular S···N contacts of 2.83 Å, giving rise to four-membered NCNS rings. During the thermolysis of **4** at 95 °C in toluene a transient species (λ_{max} 820 nm) was detected. It decomposes with second-order kinetics to give **5** (λ_{max} 450 nm). The ESR spectrum of the reaction mixture consisted of the superposition of a three-line 1:1:1 spectrum ($g = 2.0074$, $A_N = 11.45$ G), attributed to $(PhS)_2N^{\bullet}$, upon a doublet of quintets (1:2:3:2:1) with $g = 2.0070$, $A_N = 6.14$ G, $A_H = 2.1$ G assigned to the radical $HCN_2(SPh)_2^{\bullet}$. Density functional theory (DFT) calculations for the models of the radical showed the *E,Z* isomer to have the lowest energy. Thermochemical calculations indicate that the decomposition of $HCN_2(SH)_3$ into the diazene (*Z,E,Z*)-HSN═C(H)N═NC(H)═NSH (and 2 HSSH) is substantially more exothermic ($\Delta H = -176.1$ kJ mol^{-1}) than the corresponding formation of the isomeric eight-membered ring $(HC)_2N_4(SH)_2$ ($\Delta H = -40.6$ kJ mol^{-1}). These calculations also indicate that the diazene is formed by a mechanism in which the RS$^{\bullet}$ radical acts as a catalyst.

Introduction

The formation of persistent free radicals is a pervasive and fascinating feature of sulfur−nitrogen chemistry.[1] For example, at 80 °C $(PhS)_3N$ generates the purple $(PhS)_2N^{\bullet}$ radical, which decomposes to PhSSPh and N_2.[2] The dithiadiazolyl radicals RCNSSN$^{\bullet}$ (and their selenium analogues) have attracted considerable attention,[3] particularly with regard to the construction of low-dimensional molecular conductors.[4] The reactions of *N,N,N′*-tris(trimethylsilyl)benzamidine with chalcogen chlorides are a fruitful source of these five-membered rings[5] as well as the eight-membered ring $(PhC)_2N_4S_2$[6] or even the six-membered ring $Ph_2C_2HN_3SeCl_2$.[7] The treatment of the monofunctional reagents RECl (E = S, Se) with $PhCN_2(SiMe_3)_3$ (in a 3:1 molar ratio) produces the expected trisubstituted derivatives $PhCN_2(ER)_3$ initially. However, with the exception of $PhCN_2(SCCl_3)_3$,[8] such derivatives decompose to the intensely colored (dark red or purple) diazenes REN═C(Ph)N═NC(Ph)═NER of type **1**, also known as *azo dyes*.[9] The most remarkable feature of these diazenes is the weak intramolecular E---N interaction (2.65 Å in **1a**[9] and 2.61 Å in **1b**[10a]). ESR spectroscopy has provided evidence for the generation of free radicals, tentatively identified as the resonance-stabilized derivatives $PhCN_2(EPh)_2^{\bullet}$ (**2**; E = S, Se), as intermediates in the formation of the diazenes.[8] Under kinetically controlled conditions, i.e. at low temperatures, the reaction of $ArCN_2(SiMe_3)_3$ with PhSCl yields 8-membered rings of the type $(ArC)_2N_4(SPh)_2$ (**3**; R = Ph) and, in one case,

* To whom correspondence should be addressed. Tel: (403) 220-5741. Fax: (403) 289-9488. E-mail: chivers@acs.ucalgary.ca.
† The University of Calgary.
‡ University of Windsor.
⊗ Abstract published in *Advance ACS Abstracts,* May 15, 1996.

(1) Preston, K. F.; Sutcliffe, L. H. *Magn. Reson. Chem.* **1990**, *28*, 189.
(2) (a) Barton, D. H. R.; Blair, I. A.; Magnus, P. D.; Norris, R. K. *J. Chem. Soc., Perkin Trans. 1* **1973**, 1031−1037. (b) Almog, J.; Barton, D. H. R.; Magnus, P. D.; Norris, R. K. *J. Chem. Soc., Perkin Trans. 1* **1974**, 853.
(3) Banister, A. J.; Rawson, J. M. In *The Chemistry of Inorganic Ring Systems*; Steudel, R., Ed.; Elsevier: Amsterdam, 1992; Chapter 17, p 323.
(4) Cordes, A. W.; Haddon, R. C.; Oakley, R. T. In *The Chemistry of Inorganic Ring Systems*; Steudel, R., Ed.; Elsevier: Amsterdam, 1992; Chapter 17, p 295.
(5) See, for example: Del Bel Belluz, P.; Cordes, A. W.; Kristof, E. M.; Kristof, P.; Liblong, S. W.; Oakley, R. T. *J. Am. Chem. Soc.* **1989**, *111*, 9276.
(6) (a) Boeré, R. T.; Moock, K. H.; Derrick, S.; Hoogerdijk, W.; Preuss, K.; Yie, J. *Can. J. Chem.* **1993**, *71*, 473. (b) Amin, M.; Rees, C. W. *J. Chem. Soc. Chem. Commun.* **1989**, 1137.
(7) Fenske, D.; Ergezinger, C.; Dehnicke, K. *Z. Naturforsch.* **1989**, *44B*, 857.
(8) Chandrasekhar, V.; Chivers, T.; Kumaravel, S. S.; Parvez, M.; Rao, M. N. S. *Inorg. Chem.* **1991**, *30*, 4125.
(9) Chandrasekhar, V.; Chivers, T.; Fait, J. F.; Kumaravel, S. S. *J. Am. Chem. Soc.* **1990**, *112*, 5373.
(10) (a) Krouse, I. M.Sc. Thesis, The University of Calgary, 1996. (b) Zoricak, P.; Vargas-Baca, I.; Parvez, M.; Chivers, T. *Phosphorus, Sulfur Silicon Relat. Elem.* **1994**, *93/94*, 455.

S0020-1669(96)00317-5 CCC: $12.00

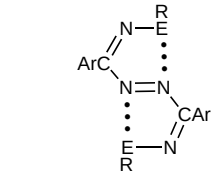

1a, (E = Se, R = Me, Ar = Ph)
1b, (E = S, R = Ar = 4-$CH_3C_6H_4$)

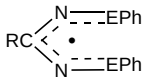

2a, R = Ph
2b, R = H

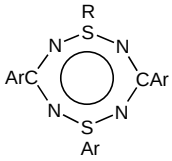

3

the 16-membered ring $(ArC)_4N_8(SPh)_4$ (Ar = 4-BrC_6H_4) has been isolated and structurally characterized.[10b]

In this work we describe the synthesis and X-ray structure of tris(thiophenolato)formamidine, $HCN_2(SPh)_3$ (**4**), whose decomposition into the corresponding diazene PhSN═C(H)N═NC(H)═NSPh (**5**) has been monitored by UV−vis, ^{1}H NMR, and ESR spectroscopy in order to provide further insight into the mechanism of the formation of the diazenes **1** and the heterocycles **3**. Interestingly, the diazene **5** is obtained in a different conformation from that found for **1b**,[10a] although it also contains S···N close contacts.

Theoretical calculations have become an important tool in the study of reaction mechanisms, including those involving sulfur-containing molecules.[11] Approximate density functional theory (DFT) provides a computationally expeditious means of modeling the properties of chalcogen−nitrogen compounds.[12] The experimental study of the decomposition of **4** has been complemented with DFT calculations to provide a thermodynamic overview of the process in terms of a mechanism involving free radicals.

Experimental Section

Reagents and General Procedures. All reactions and the manipulation of moisture-sensitive compounds were carried out under an atmosphere of dry N_2 by using Schlenk techniques or a Vacuum Atmospheres drybox. The following reagents were prepared by literature procedures: $HCN_2(SiMe_3)_3$[13] and PhSCl.[14] All solvents were dried and distilled by standard methods before use: toluene and hexanes (Na/benzophenone).

Instrumentation. Elemental analyses were obtained at the Department of Chemistry, The University of Calgary. UV−vis spectra were run on a Cary 5E spectrophotometer. IR spectra were recorded with a Mattson Instruments 4030 Galaxy Series FT-IR instrument, as Nujol mulls on KBr disks. ^{1}H NMR spectra were recorded on a Bruker ACE 200 spectrometer, and chemical shifts are reported relative to Me_4Si in CD_2Cl_2. MS (EI at 70 eV) and GC−MS were measured on a Kratos MS80RFA instrument. ESR spectra were recorded on a Bruker ESP-300e spectrometer equipped with a NMR magnetometer, a microwave counter, and a variable-temperature accessory.

Preparation of $HCN_2(SPh)_3$. A solution of PhSCl (2.45 g, 16.9 mmol) in hexanes (25 mL) was added slowly to a solution of $HCN_2(SiMe_3)_3$ (1.47 g, 5.65 mmol) in hexanes (25 mL) at −100 °C. The yellow reaction mixture was stored at −20 °C for 60 h. After removal of the solvent under vacuum, the crude product was obtained as an off-white powder, which was recrystallized from a CH_2Cl_2−hexanes mixture. The colorless crystals so obtained were washed with diethyl ether to give $HCN_2(SPh)_3$ (1.01 g, 2.97 mmol, 53%). Mp: 100 °C dec. Anal. Calcd for $C_{19}H_{16}N_2S_3$: C, 61.92; H, 4.38; N, 7.60. Found: C, 61.43; H, 4.46; N, 7.74. ^{1}H NMR (CD_2Cl_2): δ 8.18 (s, C−*H*, 1H), 7.60−7.10 (m, C_6H_5, 15H). EI-MS (*m/z*): 368 (M^+), 218 (Ph_2S_2), 109 (PhS). IR (cm^{-1}, Nujol): 1606 m, 1578 m, 1303 m, 1169 m, 1115 m, 1082 m, 1023 m, 736 s, 688 m.

Preparation of PhSN═C(H)N═NC(H)−NSPh (5). A solution of PhSCl (2.96 g, 20.5 mmol) in CH_2Cl_2 (20 mL) was added slowly to a solution of $HCN_2(SiMe_3)_3$ (1.82 g, 7.0 mmol) in CH_2Cl_2 (25 mL) at 23 °C. The mixture was heated at reflux for 18 h, and then the solvent was removed under vacuum. The red residue was recrystallized from diethyl ether at −20 °C to give a mixture of the diazene **5** and Ph_2S_2, which redissolved upon slow warming to give red crystals of PhSN═C(H)N═NC(H)═NSPh (0.21 g, 0.67 mmol, 7%). Mp: 130 °C. Anal. Calcd for $C_{14}H_{12}N_4S_2$: C, 55.98; H, 4.03; N, 18.65. Found: C, 55.97; H, 3.77; N, 18.00. IR (cm^{-1}, Nujol): 1299 m, 1156 m, 1088 m, 1079 m, 1022 m, 889 m, 800 m, 722 m, 705 m, 682 m. UV−vis (toluene, 95 °C): λ_{max} 470 nm, $\epsilon = 1.37 \times 10^4$ M^{-1} cm^{-1}.

Spectroscopic Studies of the Decomposition of $HCN_2(SPh)_3$ (4). (a) UV−vis. In a typical experiment a 10^{-3} M solution of **4** in toluene was heated at 95 °C under nitrogen. The UV−vis spectrum was recorded at regular intervals. In another experiment an excess of PhSSPh was added to the solution of **4**, prior to heating, in order to probe the effect of PhSSPh on the decomposition rate.

(b) ESR. A 10^{-3} M solution of **4** in deoxygenated toluene was stored at 0 °C prior to the recording of spectra. The solution was heated to 92 °C, and ESR spectra were acquired after 5, 10, 55, and 85 min. The solution was then cooled to 23 °C and an additional spectrum was recorded the next day.

(c) ^{1}H NMR. A 10^{-1} M solution of **4** in a deuterated solvent was kept at a constant temperature between 23 and 95 °C, and the ^{1}H NMR spectrum was monitored frequently.

X-ray Analyses. Measurements were made on a Rigaku AFC65 diffractometer with graphite-monochromated Mo K_α radiation (λ = 0.710 69 Å). The crystal data for **4** and **5** are given in Table 1. Atomic coordinates for **4** and **5** can be found in Tables 2 and 3, respectively.

Compound 4. A suitable colorless prismatic crystal of **4** (0.50 × 0.40 × 0.21 mm) was obtained by crystallization from CH_2Cl_2−hexanes at 20 °C and sealed in a glass capillary. Accurate cell dimensions and a crystal orientation matrix were determined by a least-squares refinement of the setting angles of 25 carefully centered reflections in the range $24.90 < 2\theta < 38.92°$. Intensity data were collected by the $\omega-2\theta$ scan method with a scan speed of 4.0° min^{-1} and scan width $(1.26 + 0.34 \tan\theta)°$ to a maximum 2θ value of 50.1°. The intensities of 3274 reflections were measured, of which 1761 had $I > 3.00\sigma(I)$. Over the course of data collection, the standards decreased by 6.7%. A linear correction factor was applied to the data to account for this phenomenon. The data were corrected for Lorentz and polarization effects, and an empirical absorption correction was applied. The

Table 1. Crystallographic Data for $HCN_2(SPh)_3$ (**4**) and PhSNC(H)N═NC(H)NSPh (**5**)

	4	**5**
formula	$C_{19}H_{16}N_2S_3$	$C_{14}H_{12}N_4S_2$
fw	368.53	300.40
space group	$P2_{1/a}$ (No. 14)	$P2_{1/n}$ (No. 14)
a, Å	9.874(2)	5.897(6)
b, Å	19.133(2)	18.458(10)
c, Å	10.280(2)	7.050(8)
β, deg	113.37(1)	110.97(5)
V, Å^3	1782.8(5)	716(1)
Z	4	2
T, °C	−123.0	−103.0
ρ_{calcd}, g cm^{-3}	1.373	1.392
μ, cm^{-1}	4.18	3.66
R^a	0.042	0.075
$R_w{}^b$	0.049	0.085

^{a} $R = \Sigma||F_o| - |F_c||/\Sigma|F_o|$. ^{b} $R_w = [\Sigma w\Delta^2/\Sigma wF_o{}^2]^{1/2}$.

(11) (a) Drozdova, Y.; Steudel, R. *Chem. Eur. J.* **1995**, *1*, 193. (b) Steudel, R. *Angew. Chem., Int. Ed. Engl.* **1995**, *34*, 1313.
(12) (a) Chivers, T.; McGregor, K.; Parvez, M.; Vargas-Baca, I.; Ziegler, T. *Can. J. Chem.* **1995**, *73*, 1380. (b) Chivers, T.; Jacobsen, H.; Vollmerhaus, R.; Ziegler, T. *Can. J. Chem.* **1994,** *72*, 1582.
(13) Cordes, A. W.; Bryan, C. D.; Davis, W. M.; de Laat, R. H.; Glarum, S. H.; Goddard, J. D.; Haddon, R. C.; Hicks, R. G.; Kennepohl, D. K.; Oakley, R. T.; Scott, S. R.; Westwood, N. P. C. *J. Am. Chem. Soc.* **1993**, *115*, 7232.
(14) Mueller, W. H. *J. Am. Chem. Soc.* **1968**, *90*, 2075.

Table 2. Atomic Coordinates and B_{eq} Values for **4**

atom	*x*	*y*	*z*	B_{eq}, Å^2 [a]
S(1)	0.5068(1)	0.14773(6)	0.5114(1)	2.97(2)
S(2)	0.6540(1)	0.28432(6)	0.5369(1)	3.00(3)
S(3)	0.4510(2)	0.22786(9)	0.9136(2)	3.14(4)
S(3′)	0.4442(4)	0.1160(2)	0.7755(3)	2.33(8)
N(1)	0.5655(4)	0.2241(2)	0.5980(3)	2.67(8)
N(2)	0.4892(4)	0.1999(2)	0.7829(4)	2.99(9)
C(1)	0.5371(4)	0.2421(2)	0.7169(4)	2.64(10)
C(2)	0.6683(5)	0.0956(2)	0.5726(4)	2.68(10)
C(3)	0.6694(5)	0.0394(2)	0.4870(5)	3.6(1)
C(4)	0.7930(6)	−0.0031(3)	0.5285(6)	4.5(1)
C(5)	0.9160(6)	0.0112(3)	0.6516(6)	4.4(1)
C(6)	0.9133(5)	0.0666(3)	0.7344(5)	3.9(1)
C(7)	0.7909(5)	0.1095(2)	0.6962(4)	3.3(1)
C(8)	0.5102(4)	0.3117(2)	0.3768(4)	2.43(9)
C(9)	0.5477(5)	0.3234(2)	0.2627(5)	3.5(1)
C(10)	0.4407(6)	0.3475(3)	0.1376(5)	4.5(1)
C(11)	0.2982(6)	0.3563(3)	0.1227(5)	4.4(1)
C(12)	0.2615(5)	0.3440(3)	0.2371(5)	4.2(1)
C(13)	0.3681(5)	0.3222(2)	0.3648(5)	3.5(1)
C(14)	0.3771(5)	0.1524(3)	0.9643(6)	4.4(1)
C(15)	0.3388(6)	0.1502(3)	1.0807(6)	4.8(1)
C(16)	0.2940(5)	0.0879(3)	1.1190(5)	3.9(1)
C(17)	0.2855(6)	0.0290(3)	1.0411(5)	4.2(1)
C(18)	0.3238(7)	0.0328(3)	0.9261(6)	5.2(2)
C(19)	0.3682(6)	0.0950(3)	0.8892(6)	4.7(1)
H(1)	0.5551	0.2890	0.7500	3.1597
H(3)	0.5866	0.0304	0.4012	4.3590
H(4)	0.7937	−0.0424	0.4723	5.3868
H(5)	1.0015	−0.0173	0.6780	5.3012
H(6)	0.9968	0.0757	0.8195	4.7035
H(7)	0.7906	0.1482	0.7541	3.9168
H(9)	0.6452	0.3148	0.2699	4.1502
H(10)	0.4669	0.3583	0.0604	5.3816
H(11)	0.2249	0.3707	0.0344	5.3054
H(12)	0.1627	0.3504	0.2279	5.0203
H(13)	0.3432	0.3146	0.4440	4.1446
H(15)	0.3436	0.1915	1.1338	5.7445
H(16)	0.2692	0.0861	1.1992	4.7226
H(17)	0.2537	−0.0140	1.0658	5.0136
H(18)	0.3195	−0.0080	0.8720	6.2309
H(19)	0.3925	0.0981	0.8087	5.6126

[a] $B_{eq} = {}^8/_3\pi^2(U_{11}(aa^*)^2 + U_{22}(bb^*)^2 + U_{33}(cc^*)^2 + 2U_{12}aa^*bb^*(\cos\gamma) + 2U_{13}aa^*cc^*(\cos\beta) + 2U_{23}bb^*cc^*(\cos\alpha))$.

Table 3. Atomic Coordinates and B_{eq} Values for **5**

atom	*x*	*y*	*z*	B_{eq}, Å^2 [a]
S(1)	0.5375(3)	0.08939(10)	0.6255(2)	3.53(3)
N(1)	0.9124(8)	0.0160(3)	0.9354(7)	3.3(1)
N(2)	0.7956(8)	0.0629(3)	0.6033(7)	3.5(1)
C(1)	0.9528(10)	0.0296(3)	0.7558(9)	3.6(1)
C(2)	0.3889(10)	0.1280(3)	0.3809(8)	3.1(1)
C(3)	0.4825(10)	0.1271(4)	0.2318(9)	3.6(1)
C(4)	0.3553(11)	0.1602(4)	0.0499(8)	3.9(2)
C(5)	0.1337(11)	0.1932(4)	0.0194(9)	3.8(1)
C(6)	0.0395(10)	0.1924(4)	0.1710(10)	4.2(2)
C(7)	0.1670(10)	0.1600(4)	0.3548(9)	3.4(1)
H(1)	1.1008	0.0138	0.7445	4.3146
H(3)	0.6334	0.1040	0.2522	4.2762
H(4)	0.4198	0.1604	−0.0558	4.6204
H(5)	0.0475	0.2163	−0.1063	4.5499
H(6)	−0.1136	0.2142	0.1497	4.9830
H(7)	0.1039	0.1596	0.4613	4.1130

[a] $B_{eq} = {}^8/_3\pi^2(U_{11}(aa^*)^2 + U_{22}(bb^*)^2 + U_{33}(cc^*)^2 + 2U_{12}aa^*bb^*(\cos\gamma) + 2U_{13}aa^*cc^*(\cos\beta) + 2U_{23}bb^*cc^*(\cos\alpha))$.

structure was solved by direct methods[15] and expanded using Fourier techniques.[16] The non-hydrogen atoms were refined anisotropically. One of the S atoms was disordered over the two sites S(3) and S(3)′ with site occupancy factors of 0.67(1) and 0.33(1), respectively. Hydrogen atoms were included but not refined. Refinement converged with $R = 0.042$ and $R_w = 0.049$. Scattering factors were those of Cromer and Waber,[17] and allowance was made for anomalous dispersion.[18] All calculations in this study were performed using teXsan.[19]

Compound 5. A dark brown plate of **5** (0.63 × 0.33 × 0.15 mm) was obtained by recrystallization from diethyl ether at −30 °C and mounted on a glass fiber. Cell constants and an orientation matrix for data collection were obtained by a least-squares refinement of the setting angles of 15 carefully centered reflections in the range $15.00 < 2\theta < 30.00°$: scan speed 4.0° min^{-1}, scan width $(1.78 + 0.34 \tan\theta)°$ to a maximum 2θ value of 55.1°. The data were corrected for Lorentz and polarization effects, and an empirical absorption correction was applied. The intensities of 1725 reflections were measured, of which 968 had $I > 3\sigma(I)$. No decay correction was applied. The structure was solved by direct methods[20] and expanded using Fourier techniques.[16] The non-H atoms were refined anisotropically. H atoms were included but not refined. Refinement converged with $R = 0.075$ and $R_w = 0.085$.

Computational Details

All calculations were based on approximate density functional theory (DFT) within the local density approximation,[21] using the ADF program system developed by Baerends et al.[22,23] and vectorized by Raveneck.[24] The numerical integration was based on a scheme developed by Becke.[25] All molecular dimensions were fully optimized, by a procedure based on the method developed by Versluis and Ziegler.[26] Open-shell species were optimized at the unrestricted level. All bonding energies were evaluated by the generalized transition state method of Ziegler and Rauk.[27] This treatment also allows for a detailed energy decomposition of the total bonding energy into steric and single-orbital contributions.[28] Reaction enthalpies were calculated as the difference of atomization energies between reactants and products. Zero-point energy corrections were neglected. Thus, the calculated ΔH values correspond to the electronic reaction enthalpies. A double-ζ STO basis[29] was employed for the *n*s and *n*p shells of the main-group elements. This basis was augmented by a 3d STO function for sulfur, and for hydrogen a 2p STO was used as polarization. Electrons in lower shells were treated by the frozen-core approximation.[22] A set of auxiliary[30] s, p, d, f, and g STO functions, centered on the different nuclei, was used in order to fit the molecular density and present Coulomb and exchange potentials accurately in each SCF cycle. Energy differences were calculated by augmenting the local density approximation (LDA) energy expression

(15) SAPI91: Fan Hai-Fu, Structure Analysis Programs with Intelligent Control, Rigaku Corp., Tokyo, Japan, 1991.

(16) DIRDIF94: Beurskens, P. T.; Admiraal, G.; Beurskens, G.; de Gelder, R.; Israel, R.; Smits, J. M. M. Technical Report of the Crystallography Laboratory, University of Nijmegen, Nijmegen, The Netherlands, 1994.

(17) Cromer, D. T.; Waber, J. T. *International Tables for X-ray Crystallography*; Kynoch Press: Birmingham, England, 1974; Vol. IV, Table 2-2A.

(18) Ibers, J. A.; Hamilton, W. C. *Acta Crystallogr.* **1964**, *17*, 781.

(19) teXsan: Crystal Structure Analysis Package, Molecular Structure Corp., 1985 and 1992.

(20) SIR92: Altomare, A.; Burla, M. C.; Camalli, M.; Cascarano, M.; Giacovazzo, C.; Guagliardi, A.; Polidori, G. *J. Appl. Crystallogr.*, manuscript in preparation.

(21) (a) Gunnarsson, O.; Lundquist, I. *Phys. Rev.* **1974**, *B10*, 1319. (b) Gunnarsson, O.; Lundquist, I. *Phys. Rev.* **1976**, *B13*, 4274. (c) Gunnarsson, O.; Johnson, M.; Lundquist, I. *Phys. Rev.* **1979**, *B20*, 3136.

(22) Baerends, E. J.; Ellis, D. E.; Ros, P. *Chem. Phys.* **1973**, *2*, 41.

(23) Baerends, E. J. Ph.D. Thesis, Frije Universiteit, Amsterdam, 1975.

(24) Ravenek, W. In *Algorithms and Applications on Vector and Parallel Computers*; Riele, H. J. J., Dekker, Th. J., van de Horst, H. A., Eds.; Elsevier: Amsterdam, 1987.

(25) Becke, A. D. *J. Chem. Phys.* **1988**, *88*, 2547.

(26) Versluis, L.; Ziegler, T. *J. Chem. Phys.* **1988**, *88*, 322.

(27) Ziegler, T.; Rauk, A. *Theor. Chim. Acta* **1977**, *46*, 1.

(28) Ziegler, T. In *Metal-Ligand Interactions: from Atoms, to Clusters, to Surfaces*; Salahub, D. R., Russo, N., Eds.; Kluwer Academic: Amsterdam, 1992.

(29) (a) Snijders, J. G.; Baerends, E. J.; Vernoijs, P. *At. Nucl. Data Tables* **1982**, *26*, 483. (b) Vernoijs, P.; Snijders, J. G.; Baerends, E. J. *Slater Type Basis Functions for the Whole Periodic System, Internal Report*; Frije Universiteit, Amsterdam, 1981.

(30) Krijn, J.; Baerends, E. J. *Fitfunctions in the HFS Method, Internal Report*; Frije Universiteit, Amsterdam, 1984.

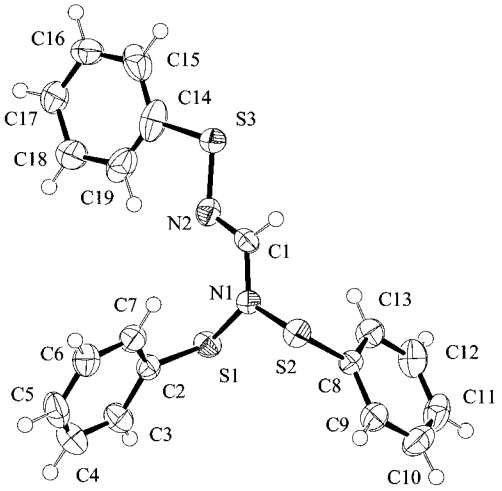

Figure 1. ORTEP drawing for $HCN_2(SPh)_3$ (**4**).

by Vosko et al.[31] with Becke's[32] exchange corrections and Perdew's nonlocal correlation correction.[33]

The following model structures were fully optimized: $HCN_2(SH)_3$, HSNC(H)N(SH)N(SH)C(H)NSH, HSNC(H)N•N(SH)C(H)NSH, (*Z*,*E*,*Z*)-HSN═C(H)N═NC(H)═NSH, $(HC)_2N_4(SH)_2$, *trans*-HN═NH, HSSH, HN•SH, HS(H)NN(H)SH, $(HS)_2N$•, HCN, and HS•. The disulfides HSSH and $(HS)_2N$• were assumed to have C_2 geometry; a C_{2h} symmetry was used for (*Z*,*E*,*Z*)-HSN═C(H)N═NC(H)═NSH and *trans*-HN═NH. The eight-membered ring $(HC)_2N_4(SH)_2$, an isomer of the (*Z*,*E*,*Z*)-diazene, was calculated on the basis of the C_{2v} geometry obtained from a preliminary structure determination of $(4\text{-}BrC_6H_4C)_2N_4(SPh)_2$.[34] A thorough study of the structure of $HCN_2(SH)_2$• was also carried out, and the most stable geometry was considered for the thermodynamic analysis. All other structures were calculated assuming no symmetry constraints.

Results and Discussion

Synthesis and X-ray Structure of $HCN_2(SPh)_3$. Tris(phenylthio)formamidine, $HCN_2(SPh)_3$ (**4**), is readily prepared from the reaction of $HCN_2(SiMe_3)_3$ with 3 molar equiv of PhSCl in hexanes at −100 °C. The product was isolated in 53% yield as white crystals, usually tainted with the red diazene PhSN═C(H)N═NC(H)═NSPh (**5**), which is formed by the thermal decomposition of **4** in the solid state or, more rapidly, in solution (*vide infra*). It is necessary to store **4** at low temperature (−20 °C) to prevent this decomposition. Nevertheless, crystals of **4** suitable for an X-ray structural determination were obtained by recrystallization from diethyl ether at −20 °C. An ORTEP drawing of **4** with the atomic numbering scheme is displayed in Figure 1. Selected bond lengths and bond angles are given in Table 4. The three-coordinate nitrogen atom adopts a planar geometry ($\sum\hat{N}$ (1) = 359.9°), and the dihedral angles involving C(1)−N(1) as the central bond indicate a tendency toward planarity (∠N(2)−C(1)−N(1)−S(1) = 12.3(5)°, ∠N(2)−C(1)−N(1)−S(2) = −171.1(3)°). Nevertheless, the C(1)−N(1) bond distance of 1.401(5) Å (cf. *d*[C(1)−N(2)] = 1.261(5) Å) indicates only limited π-contributions. The N(1)−S(1) and N(1)−S(2) distances of 1.691(3) and 1.709(3) Å, respectively, are close to the mean value of 1.699 Å found for $(PhS)_3N$[35] and the corresponding S−N bond lengths of 1.694(4) and 1.700(3) Å reported for $PhCN_2(SCCl_3)_3$, which, however, is stable up to 140 °C.[8] Because of the disorder involving S(3) (see Experimental Section) it is imprudent to comment on the structural parameters involving this sulfur atom. However, the weighted average of the S(3)−N(2) distances is 1.635(5) Å, indicating a significantly shorter and, presumably, stronger S−N bond for the imido compared to the amido N atom.

Table 4. Selected Bond Lengths (Å) and Bond Angles (deg) for $HCN_2(SPh)_3$ (**4**)[a]

Bond Lengths			
S(1)−N(1)	1.691(3)	S(2)−C(14)	1.786(5)
S(1)−C(2)	1.772(4)	S(3)′−N(2)	1.660(5)
S(2)−N(1)	1.709(3)	S(3)′−C(19)	1.669(6)
S(2)−C(8)	1.773(4)	N(1)−C(1)	1.401(5)
S(3)−N(2)	1.623(4)	N(2)−C(1)	1.261(5)
Bond Angles			
N(1)−S(1)−C(2)	103.1(2)	S(2)−N(1)−C(1)	117.7(3)
N(1)−S(2)−C(8)	101.7(2)	S(3)−N(2)−S(3)′	102.2(2)
N(2)−S(13)−C(14)	103.4(3)	S(3)−N(2)−C(1)	119.6(3)
N(2)−S(3)′−C(19)	112.8(3)	S(3)′−N(2)−C(1)	138.2(3)
S(1)−N(1)−S(2)	120.5(2)	N(1)−C(1)−N(2)	124.1(4)
S(1)−N(1)−C(1)	121.7(3)		

[a] S(3) and S(3)′ represent the disordered S atom with occupancy factors of 0.67(1) and 0.33(1) Å, respectively.

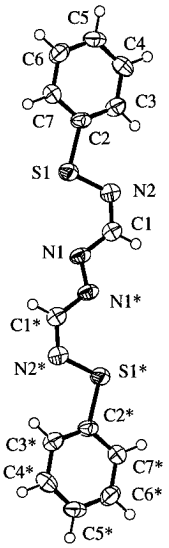

Figure 2. ORTEP drawing for PhSN═C(H)N═NC(H)═NSPh (**5**). Starred atoms are related to the unstarred atoms by the symmetry operation $-x + z$, $-y$, $-z + 2$.

Synthesis and X-ray Structure of PhSN═C(H)N═NC(H)═NSPh (5). The dark red diazene PhSN═C(H)N═NC(H)═NSPh (**5**; λ_{max} 470 nm, $\epsilon = 1.4 \times 10^4$ M^{-1} cm^{-1}) was obtained by the *in situ* decomposition of **4** in boiling CH_2Cl_2. Chromatography on silica gel has been successful for the separation of diazenes of the type **1** and the corresponding 8- and 16-membered rings.[10b,34] In the present case there was no evidence for the formation of a $C_2N_4S_2$ heterocycle, but the attempted purification of **5** by chromatography on silica gel resulted in hydrolysis. Eventually, however, a pure sample of **5** was obtained in *ca*. 7% yield by recrystallization from diethyl ether. The low yield is partly the result of the similar solubilities of **5** and the byproduct Ph_2S_2 in organic solvents.

An X-ray structural determination of **5** revealed the *Z*,*E*,*Z* isomer depicted in Figure 2. Selected bond lengths and bond angles are given in Table 5. The eight-atom SNCNNCNS chain is essentially planar, with the two phenyl groups tilted only slightly with respect to this chain (the torsion angles N(2)−S(1)−C(2)−C(3) and N(2)−S(1)−C(2)−C(7) are 3.5(6) and −176.2(5)°, respectively). The packing of this planar molecule in the unit cell is illustrated in Figure 3. There are no significant

(31) Vosko, S. H.; Wilk, L.; Nusair, M. *Can. J. Phys.* **1990**, *58*, 1200.
(32) Becke, A. D. *Phys. Rev.* **1988**, *A38*, 2938.
(33) (a) Perdew, J. P. *Phys. Rev.* **1986**, *B33*, 8822. (b) Perdew, J. P. *Phys. Rev.* **1986**, *B34*, 7406.
(34) Chivers, T.; Parvez, M.; Zoricak, P. Unpublished results.
(35) Carruthers, J. R.; Prout, K.; Watkin, D. J. *Cryst. Struct. Commun.* **1981**, *10*, 1217.

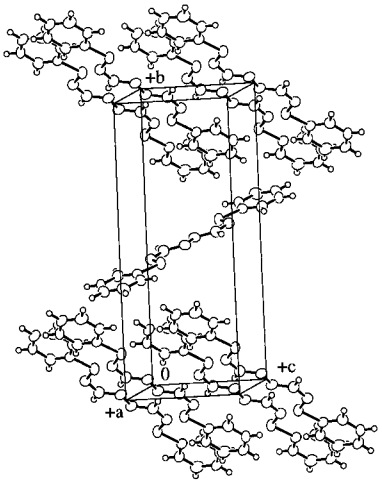

Figure 3. Packing diagram for PhSN═C(H)N═NC(H)═NSPh (**5**).

Table 5. Selected Bond Lengths (Å), Bond Angles (deg), and Torsion Angles (deg) for PhSNC(H)N═NC(H)NSPh (**5**)

Bond Lengths			
S(1)−N(2)	1.658(5)	N(1)−C(1)	1.392(7)
S(1)−C(2)	1.780(5)	N(2)−C(1)	1.296(7)
N(1)−N(1)*	1.254(8)		
Bond Angles			
N(1)−S(1)−C(2)	100.2(3)	S(1)−N(2)−C(1)	118.0(4)
N(1)*−N(1)−C(1)	112.4(6)	N(1)−C(1)−N(2)	122.4(5)
Torsion Angles			
S(1)−N(2)−C(1)−N(1)		−0.5(9)	
N(1)*−N(1)−C(1)−N(2)		179.2(6)	
N(2)−S(1)−C(2)−C(3)		3.5(6)	
N(2)−S(1)−C(2)−C(7)		−176.2(5)	
C(1)*−N(1)*−N(1)−C(1)		180.0	
C(1)−N(2)−S(1)−C(2)		−178.2(5)	

intermolecular interactions. The C−N bond lengths of 1.392(7) [C(1)−N(1)] and 1.296(7) Å [C(1)−N(2)] and the N═N bond distance of 1.254(8) Å (*cf.* a mean value of 1.22 Å for *trans*-diazenes)[36] indicate only modest delocalization along the diazene chain. The S(1)−N(2) distance of 1.658(5) Å is significantly shorter than the single-bond value of 1.710 Å for an sp^2 N atom.[36] The most interesting feature of the structure of **5** is the nature of the intramolecular S(1)···N(1) interaction. Like **1a** and **1b**, the diazene **5** is a *Z*,*E*,*Z* isomer with respect to the N═C, N═N, and C═N bonds. However, the formamidine derivative **5** is a rotamer of the diazenes exemplified by **1a** and **1b** with respect to rotation about the C−N single bond. Consequently, the weak intramolecular S···N interaction in **5** (d(S···N) = 2.83 Å) results in the formation of a four-membered NCNS ring, whereas the corresponding contact in **1b** gives rise to five-membered NNCNS rings with a stronger S···N interaction (2.61 Å).[10a]

Thermodynamics of the Formation of Diazenes and Cyclic Products. In a previous report we have proposed that the formation of diazenes of type **1** from $ArCN_2(SPh)_3$ occurs via the resonance-stabilized radicals **2**.[8] In this work we provide a thermodynamic analysis of each step in the process based on DFT calculations.

The formation of both the diazene and the eight-membered ring is exothermic (eqs 1 and 2). However, since two S−N bonds are weaker than the N═N bond, diazene formation is favored:

$$2HCN_2(SH)_3 \rightarrow HSN{=}C(H)N{=}NC(H){=}NSH + 2HSSH \quad (1)$$

$$\Delta H = -176.1 \text{ kJ mol}^{-1}$$

$$2HCN_2(SH)_3 \rightarrow (HC)_2N_4(SH)_2 + 2HSSH \quad (2)$$

$$\Delta H = -40.6 \text{ kJ mol}^{-1}$$

The generation of the radical $HC(NSH)_2^{\bullet}$ requires an endothermic step, i.e. homolytic cleavage of an S−N bond. Homolysis of the (longer) S−N(amino) bond (eq 3a) should occur preferentially, since it is less endothermic than cleavage of the S−N(imino) bond (eq 3b):

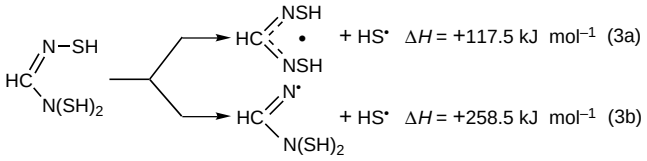

The imino radical is unstable with respect to fragmentation into HCN and $(HS)_2N^{\bullet}$ (eq 4):

$$HC[N(SH)_2]N^{\bullet} \rightarrow HCN + (HS)_2N^{\bullet} \quad (4)$$

$$\Delta H = -51.0 \text{ kJ mol}^{-1}$$

The formation of HSSH is a strong driving force (eq 5) (*cf.* $\Delta H = -285 \pm 11$ kJ mol^{-1} for the dimerization of RS$^{\bullet}$ (R = alkyl) and ΔH −262 kJ mol^{-1} in the case of HS$^{\bullet}$),[37] which makes the process shown in eq 6 exothermic. It can be regarded as dissociation (eq 3a) followed by abstraction (eq 7):

$$2HS^{\bullet} \rightarrow HSSH \quad (5)$$

$$\Delta H = -283.0 \text{ kJ mol}^{-}$$

$$2HCN_2(SH)_3 \rightarrow 2HC(NSH)_2^{\bullet} + 2HSSH \quad (6)$$

$$\Delta H = -48.0 \text{ kJ mol}^{-1}$$

$$HS^{\bullet} + HCN_2(SH)_3 \rightarrow HC(NSH)_2^{\bullet} + HSSH \quad (7)$$

$$\Delta H = -165.5 \text{ kJ mol}^{-1}$$

Diazene formation from the intermediate radical is still a very exothermic process (eq 8), but ring formation is not (eq 9). This indicates that, as suggested previously,[8] the formation of cyclic products from $RCN_2(SPh)_3$ does not proceed by a radical pathway:

$$2HC(NSH)_2^{\bullet} \rightarrow HSN{=}C(H)N{=}NC(H){=}NSH + HSSH \quad (8)$$

$$\Delta H = -128.1 \text{ kJ mol}^{-1}$$

$$2HC(NSH)_2^{\bullet} \rightarrow (HC)_2N_4(SH)_2 + HSSH \quad (9)$$

(36) Allen, F. H.; Kennard, O.; Watson, D. G.; Brammer, L.; Orpen, A. G.; Taylor, R. *J. Chem. Soc., Perkin Trans. 2* **1987**, S1.

(37) Griller, D.; Martinho-Simões, J. A.; Wagner, D. D. M. In *Sulfur Centered Reactive Intermediates in Chemistry and Biology*; Chatgilialoglu, C., Asmus, K. D., Eds.; Plenum Press: New York, 1990.

$$\Delta H = +74.0 \text{ kJ mol}^{-1}$$

Dimerization of the intermediate radical should occur by N−N bond formation to give a hydrazine derivative (eq 10):

$$2HC(NSH)_2^{\bullet} \rightarrow HSNC(H)N(SH)N(SH)C(H)NSH \quad (10)$$

$$\Delta H = -16.8 \text{ kJ mol}^{-1}$$

This dimer is closely related to those formed from radicals of the ArN̈SAr type,[38,39] which yield diazenes among other decomposition products.[38b] Although diazene formation (eq 11) is exothermic, it cannot occur in a concerted step (eq 13), because such a four-center process is symmetry-forbidden. Consequently, a sequence of two steps (eqs 12 and 13) must be involved:

$$2HN^{\bullet}SH \rightarrow \textit{trans}\text{-}HN{=}NH + HSSH \quad (11)$$

$$\Delta H = -163.1 \text{ kJ mol}^{-1}$$

$$2HN^{\bullet}SH \rightarrow HS(H)NN(H)SH \quad (12)$$

$$\Delta H = -138.5 \text{ kJ mol}^{-1}$$

$$HS(H)NN(H)\text{-}SH \rightarrow \textit{trans}\text{-}HN{=}NH + HSSH \quad (13)$$

$$\Delta H = -24.6 \text{ kJ mol}^{-1}$$

It is proposed, therefore, that formation of the diazene from the hydrazine derivative occurs through a hydrazinyl radical (eqs 14 and 15), in a sequence analogous to that shown in eqs 3a and 7:

$$HSNC(H)N(SH)N(SH)C(H)NSH \rightarrow HSNC(H)N(SH)N^{\bullet}C(H)NSH + HS^{\bullet} \quad (14)$$

$$\Delta H = +67.0 \text{ kJ mol}^{-1}$$

$$HS^{\bullet} + HSNC(H)N(SH)N(SH)C(H)NSH \rightarrow HSNC(H)N(SH)N^{\bullet}C(H)NSH + HSSH \quad (15)$$

$$\Delta H = -216.0 \text{ kJ mol}^{-1}$$

The loss of HS$^{\bullet}$ from this radical (eq 16) would account for the formation of a diazene in a process that is well-known in carbon chemistry.[40] Alternatively, the diazene could be formed by an abstraction process (eq 17)

$$HSNC(H)N(SH)N^{\bullet}C(H)NSH \rightarrow HSN{=}C(H)N{=}NC(H){=}NSH + HS^{\bullet} \quad (16)$$

$$\Delta H = +104.7 \text{ kJ mol}^{-1}$$

$$HS^{\bullet} + HSNC(H)N(SH)N^{\bullet}C(H)NSH \rightarrow HSNC(H)N(SH)N^{\bullet}C(H)NSH + HSSH \quad (17)$$

$$\Delta H = -178.3 \text{ kJ mol}^{-1}$$

Consideration of the various processes involved in eqs 1−17 leads to the general conclusion that, while most of the steps are exothermic, those that involve homolysis of the S−N bond are strongly endothermic. The endothermic steps must be facilitated in some way, and HS$^{\bullet}$ seems to be the most likely catalytic species. In fact, the mechanism of diazene formation would involve a radical chain process (Scheme 1) if the availability of the chain propagator was not drastically reduced by dimerization (eq 5).

Scheme 1. Proposed Radical Mechanism for the Formation of the Diazene HSNC(H)N=N(H)CNSH

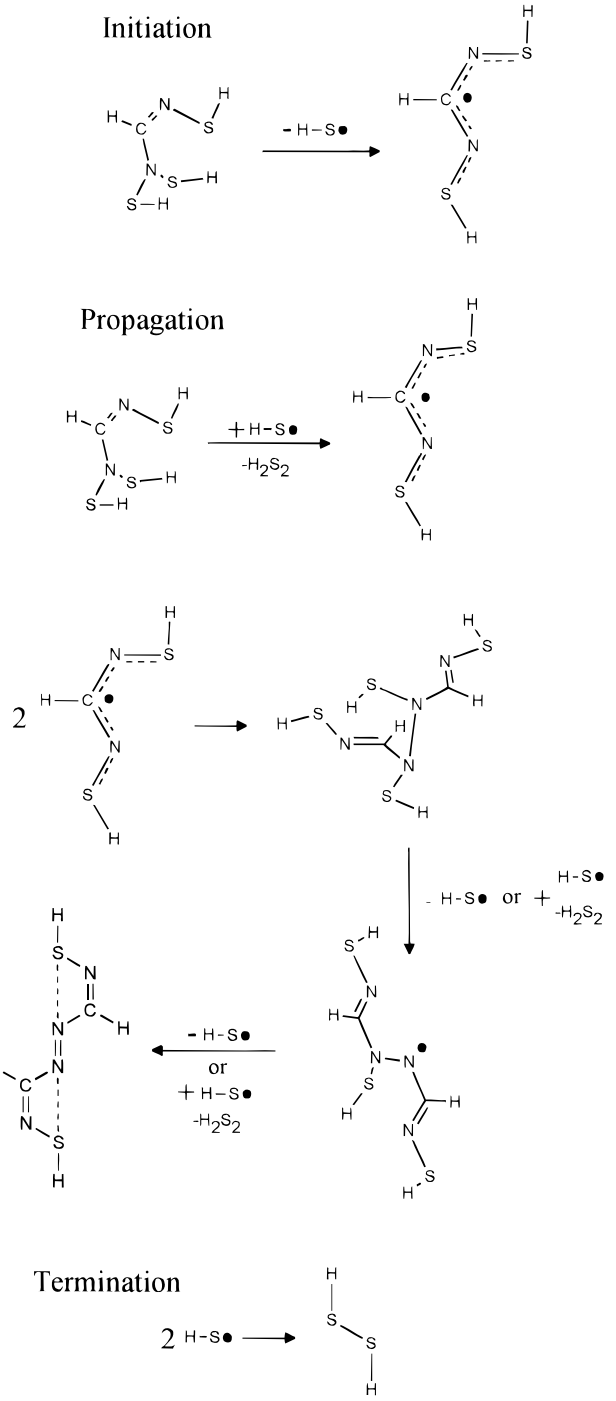

Spectroscopic Studies of the Decomposition of $HCN_2(SPh)_3$. The trithiolated formamidine $HCN_2(SPh)_3$ (**4**) decomposes into the red diazene PhSNC(H)N=NC(H)NSPh (**5**) in solution. The initial stages of the decomposition of a solution of **4** in toluene at 95 °C have been monitored by UV−visible

(38) (a) Miura, Y.; Yamamoto, A.; Katsura, Y.; Kinoshita, M. *J. Org. Chem.* **1982**, *47*, 2618. (b) Miura, Y.; Yamamoto, A.; Katsura, Y.; Kinoshita, M. *Bull. Chem. Soc. Jpn.* **1981**, *54*, 3215.

(39) Levchenko, E. S.; Dubinina, T. N.; Sereda, S. V.; Antipin, M. Yu.; Struchkov, Yu. T.; Boldeskul, I. E. *Zh. Org. Khim.* **1987**, *23*, 86.

(40) Lazar, M.; Rychly, J.; Klimo, V.; Pelikán, P.; Volko, L. *Free Radicals in Chemistry and Biology*; CRC Press: Boca Raton, FL, 1989; Chapter 3.

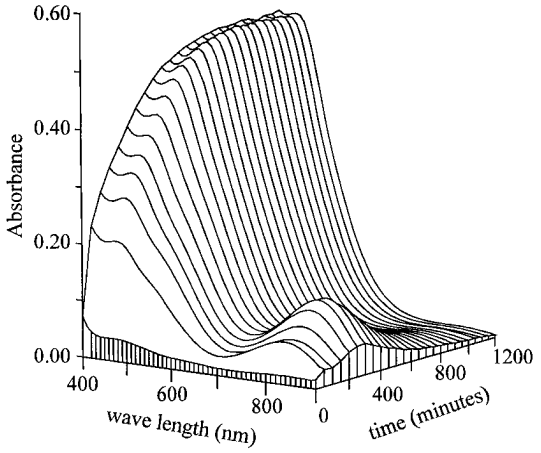

Figure 4. Evolution of the absorption spectrum during the decomposition of $HCN_2(SPh)_3$ in toluene solution.

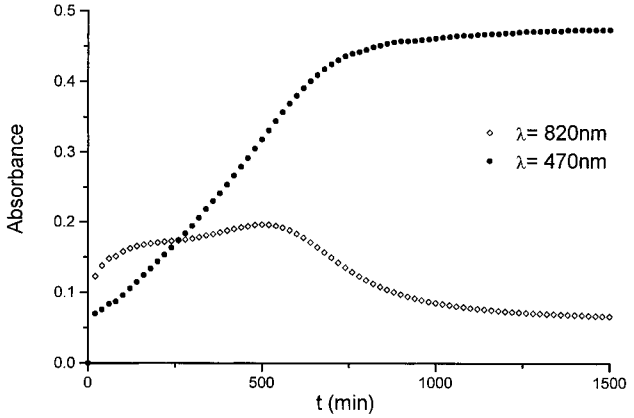

Figure 5. Time dependence of the absorbances at 820 and 450 nm during the decomposition of $HCN_2(SPh)_3$ in toluene solution.

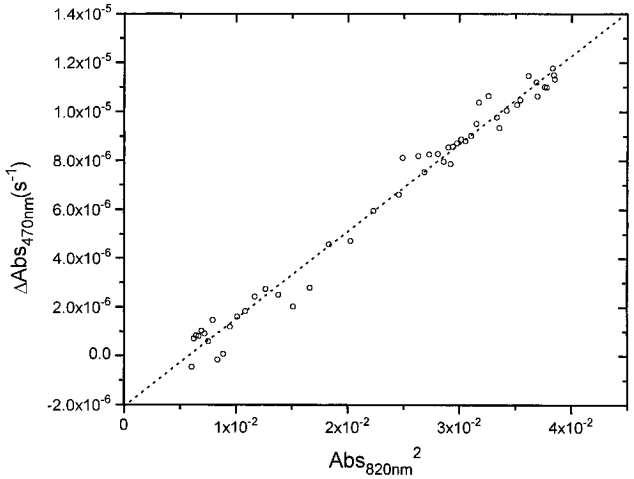

Figure 6. Dependence of the slope of $\Delta Abs_{450\ nm}$ on $Abs_{820\ nm}$ during the decomposition of $HCN_2(SPh)_3$ (1.4×10^{-4} M) in toluene solution at 95 °C ($r = 0.991$; slope $(3.6 \pm 0.1) \times 10^{-4}$ s^{-1}; y intercept $(-2.1 \pm 0.4) \times 10^{-6}$ s^{-1}).

spectroscopy, which revealed complicated kinetics. The formation of **5** was manifested by the continuous increase of the absorbance between 450 and 500 mm. Absorption by a transient species was observed at 820 nm, and no other absorption maxima were detected (Figure 4). The reaction is slow; less than 5% conversion is achieved in 20 h, and then the rate of reaction becomes even slower. Small increases of the absorbance attributable to **5** were still detectable in the following 8 h. The limited solubility of **4** in toluene precluded using higher concentrations to increase the reaction rate. We note, however,

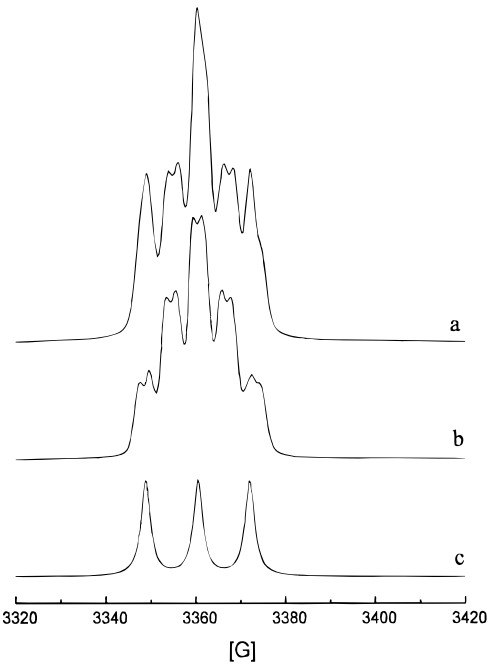

Figure 7. (a) Integrated (absorption) ESR spectrum for the decomposition of $HCN_2(SPh)_3$ in toluene solution. (b) Difference spectrum. (c) Calculated three-line spectrum.

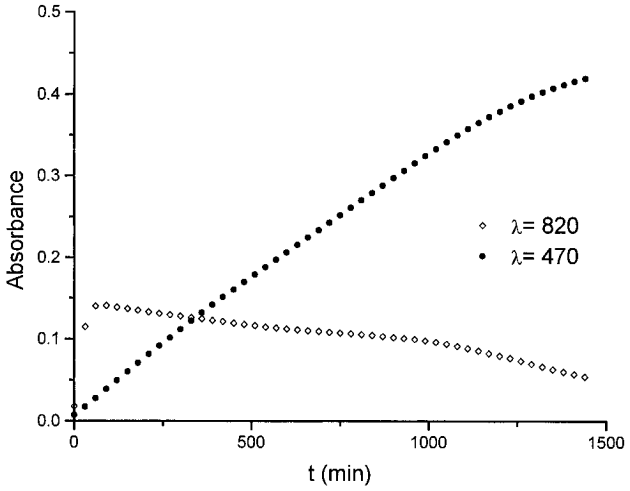

Figure 8. Time dependence of the absorbances at 820 and 450 nm of the mixture of $HCN_2(SPh)_3$ (1.4×10^{-4} M) and PhSSPh (1.3×10^{-3} M) in toluene solution at 95 °C.

that the decomposition of **4** is much faster if PhSCl is present in the reaction mixture (*vide infra*). Both absorptions at 470 and 820 nm showed a complex dependence on time (Figure 5), which prevented a more detailed kinetic study. The slope of the absorbance at 470 nm ($\Delta Abs_{470\ nm} = [Abs_{470\ nm,t} - Abs_{470\ nm,t\ -\ 1200s}]/1200$ s) is correlated with the square of the absorbance at 820 nm (Figure 6). This suggests that the transient species is an intermediate that yields **5** with second-order kinetics. The negative y intercept may indicate some reversible character of that step.

In order to characterize any radical species formed in the decomposition of **4** in hot toluene, ESR spectra were recorded at various time intervals. Initially the solution had a pale red color and gave a weak ESR spectrum. After heating, the solution was dark red and the intensity of the signal increased by 1 order of magnitude. The strongest signal was obtained at 55 min. This spectrum was integrated to give the absorption spectrum shown in Figure 7. A three-line spectrum was calculated (Figure 7c) and subtracted from the experimental

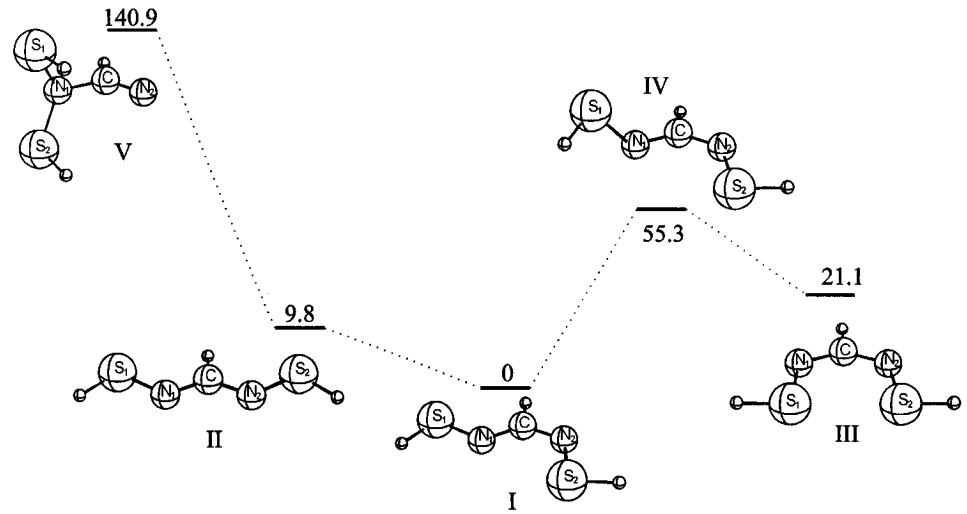

Figure 9. Potential energy diagram for the isomers of $HC(NSH)_2^{\bullet}$. Relative energy differences are given in kJ mol^{-1}. Bond distances (Å) and bond angles (deg) are as follows. **I:** C−N_1 = 1.310, C−N_2 = 1.319, N_1−S_1 = 1.665, N_2−S_2 = 1.665; N_1−C−N_2 = 123.5, S_1−N_1−C = 117.2, S_2−N_2−C = 117.2. **II:** C−N_1 = 1.317, N_1−S_1 = 1.663; N_1−C−N_2 = 119.6, S_1−N_1−C = 114.6. **III:** C−N_1 = 1.321, N_1−S_1 = 1.667; N_1−C−N_2 = 135.0, S_1−N_1−C = 119.4. **IV:** C−N_1 = 1.364, C−N_2 = 1.283, N_1−S_1 = 1.630, N_2−S_2 = 1.711; N_1−C−N_2 = 124.3, S_1−N_1−C = 120.0, S_2−N_2−C = 115.4. **V**: C−N_1 = 1.450, C−N_2 = 1.235, N_1−S_1 = 1.709; N_1−C−N_2 = 120.9, S_1−N_1−C = 115.5, S_1−N_1−S_2 = 123.4.

spectrum to give a difference spectrum consisting of a quintet of doublets (Figure 7b). The ESR spectrum recorded on the next day was very weak. The three-line spectrum corresponds to a species with a single ^{14}N coupling (g = 2.0074, A_N = 11.45 G) and no proton splitting. The ESR parameters reported for $(PhS)_2N^{\bullet}$ in benzene are g = 2.0077 and A_N = 11.5 G.[41] Consequently, we attribute the three-line spectrum to this well-known radical. The five-line spectrum belongs to a free radical with a splitting by two equivalent N atoms plus a small doublet splitting from one proton (g = 2.0070, A_N = 6.14 G, A_H = 2.1 G). Extensive ESR studies of hydrazinyl radicals have shown that, despite the nonequivalence of the two nitrogen atoms, the spectra exhibit approximate five-line patterns.[42] However, the hydrazinyl radical proposed as an intermediate in the decomposition of **4** (eqs 14 and 15) should also exhibit coupling to two inequivalent protons. The observed five-line spectrum is, therefore, attributed to the radical $HC(NSPh)_2^{\bullet}$.

Although more concentrated solutions of **4** (∼0.1 M) quickly acquire an intense red color, ^1H NMR spectra demonstrated that the process is still slow. The decomposition of **4** in CD_2Cl_2 solution at 40 °C was monitored by ^1H NMR. After 11 days, the apparent intensity ratio of the HC singlet (δ 8.18 ppm) to the aromatic multiplet at δ 7.1−7.6 ppm decreases from 1:15 to 1:120.

Up to this point, the thermolysis of **4** does not explain by itself why the diazenes are easily formed from the mixture of $RCN_2(SiMe_3)_3$ and ArSCl even at low temperatures. The thermodynamic study suggests that the process is slow due to the strongly endothermic nature of the steps that involve homolysis of the S−N bond. The key factor appears to be the availability of $PhS^{\bullet}$, which may catalyze the decomposition of $HCN_2(SPh)_3$. In any case the amounts of phenylthiyl radical present in the reaction medium must be very small. A sample of $HCN_2(SPh)_3$ was refluxed in toluene for 20 h; after removal of the solvent, GC−MS of the residue showed the presence of small amounts of 4-$CH_3C_6H_4SPh$, presumably formed by reaction of the solvent with $PhS^{\bullet}$. The effect of $PhS^{\bullet}$ could be inferred by studying the influence of other components of the reaction mixture. It was observed that the beginning of the thermolysis process is slower in the presence of an excess of PhSSPh (Figure 8). Disulfides effectively reduce the amount of $RS^{\bullet}$ by formation of the adduct $R_3S_3^{\bullet}$.[43] The structures of these radicals are unknown, but the corresponding cations $R_3S_3^+$ have been structurally characterized.[44] On the other hand, an excess of PhSC1 (2.6:1) accelerates remarkably the decomposition of **4** in $CDC1_3$ (0.14 M). At room temperature ^1H NMR shows that the decomposition is complete in 30 min. PhSCl can be regarded as a source of the $PhS^{\bullet}$ radicals that catalyze the reaction.[45]

Theoretical Calculations: Structure and Absorption Spectra of $HC(NSH)_2^{\bullet}$. ESR studies of the decomposition of $RCN_2(SPh)_3$ (R = H, Ph) in this work and a previous investigation[8] have consistently afforded evidence for the formation of the resonance-stabilized radicals $RC(NSPh)_2^{\bullet}$, but no examples of such species have been isolated and characterized. Consequently, we have obtained optimized structures of various isomers of the model radical $HC(NSH)_2^{\bullet}$ by using density functional theory (DFT) calculations in order to provide an understanding of their properties.

The relative energies of the five structural isomers considered for $HC(NSH)_2^{\bullet}$ are depicted in Figure 9. The three planar, π-delocalized structures **I** (C_s), **II** (C_{2v}), and **III** (C_{2v}) are more stable than the imido isomer **V**. The most stable π-radical (**I**) has *E*,*Z* geometry. The relatively small energy differences suggest that an equilibrium between **I**, **II**, and **III** is feasible. Structural interconversion involves rotation of the S−N bond; the transition state (**IV**) between **I** and **III** was optimized in order to evaluate the height of the barrier, which is indeed small enough to permit dynamic equilibrium. These results are

(41) Mayer, R.; Decker, D.; Bleisch, S.; Domschke, G. *J. Prakt. Chem.* **1987**, 329, 81.
(42) (a) Negareche, M.; Badrudin, Y.; Berchadsky, Y.; Friedmann, A.; Tordo, P. *J. Org. Chem.* **1986**, *51*, 342. (b) Malatesta, V.; Ingold, K. U. *J. Am. Chem. Soc.* **1973**, *95*, 6110. (c) Lunazzi, L.; Ingold, K. U. *J. Am. Chem. Soc.* **1974**, 96, 5558. (d) Malatesta, V.; Ingold, K. U. *J. Am. Chem. Soc.* **1974**, *96*, 3949. (e) Malatesta, V., Lindsay, D.; Horseville, E. C.; Ingold, K. U. *Can. J. Chem.* **1974**, *52*, 864.
(43) (a) Bonifacic, M.; Asmus, K.-D. *J. Phys. Chem.* **1984**, *88*, 6286. (b) Burkey, T. J.; Griller, D. *J. Am. Chem. Soc.* **1985**, *107*, 246.
(44) (a) Laitinen, R.; Steudel, R.; Weiss, R. *J. Chem. Soc., Dalton Trans.* **1986**, 1095. (b) Minkwitz, R.; Gerhard, V.; Krause, R.; Prenzel, H.; Preut, H. *Z. Anorg. Allg. Chem.* **1988**, *559*, 154. (c) Minkwitz, R.; Krause, R.; Preut, H. *Z. Anorg. Allg. Chem.* **1989**, *571*, 133.
(45) Russ, C. R.; Douglass, I. B. In *Sulfur in Organic and Inorganic Chemistry*; Senning, A., Ed.; Marcel Dekker: New York, 1971; p 248.
(46) Raghavachari, K.; Haddon, R. C. *J. Phys. Chem.* **1983**, *87*, 1312.

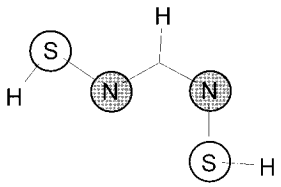

Figure 10. SOMO for $HC(NSH)_2^{\bullet}$.

reminiscent of the well-established behavior of sulfur diimides, RN═S═NR, for which the *E*,*Z* isomer is usually the most stable structural entity.[46]

The isomers **I**, **II**, and **III** have a SOMO which is a π^*_{N-S} orbital with a nodal plane on carbon (Figure 10). The coefficients of the p_z orbitals of the nitrogen atoms are nearly constant from one geometry to another. Thus, the A_N coefficients are expected to have the same value and the isomer **I** would provide an almost symmetrical five-line ESR spectrum despite the inequivalence of the N atoms.

The calculated energy for the first electronic transition, HOMO(3a″) → SOMO(4a″), for structure **I** is 1.78 eV (702 nm), close to 1.51 eV (820 nm) for the observed absorbance of the transient species in the UV−vis spectra; the 0.27 eV difference is within the limits of accuracy of DFT calculations. The transient species is, therefore, identified as $HCN(SPh)_2^{\bullet}$. The second-order rate law for the decay of this radical indicates that the dimerization equilibrium is negligible. It is a slow process, possibly due to steric hindrance, but the diazene is produced quickly once the dimer is formed.

Conclusions. Spectroscopic investigations and thermochemical calculations of the decomposition of trithiolated formamidines $HCN_2(SR)_3$ (R = Ph, H) indicate that the formation of the diazenes RSN═C(H)N═NC(H)═NSR occurs via a radical process. The initiation step involves the production of the radicals $HCN_2(SR)_2^{\bullet}$, which dimerize slowly and then quickly form the corresponding diazenes. Inhibition and catalysis by PhSSPh and PhSCl, respectively, are consistent with the role of the radical $PhS^{\bullet}$ as a catalyst. The radical $HCN_2(SR)_2^{\bullet}$ was identified by ESR and UV−vis spectra. The thermochemical calculations also indicate that the formation of eight-membered $C_2N_4S_2$ rings (or larger ring systems) from the decomposition of $ArCN_2(SPh)_3$ (Ar = aryl) does not proceed by a pathway involving $ArCN_2(SPh)_2^{\bullet}$ radicals.

Acknowledgment. We thank the Natural Sciences and Engineering Council of Canada for financial support and Dr. D. A. Armstrong for helpful comments.

Supporting Information Available: Tables giving X-ray experimental details, atomic coordinates and isotropic thermal parameters for all atoms, bond distances, bond angles, anisotropic thermal parameters, and torsion angles for **4** and **5** and a table of total atomization energies (14 pages). Ordering information is given on any masthead page.

IC960317T